Sl. No.	IIT Ropar List of Recent Publications with Abstract Coverage: December, 2025
A	**Book Chapter(s)**
1.	Catalytic pyrolysis and reforming of agro-waste for hydrogen production **PP Singh, A Goyal, A Jaswal, T Mondal** - Biohydrogen Production: Book Chapter, 2025 **Abstract:** The escalating depletion of fossil fuel reserves and the concurrent rise in waste generation have intensified global challenges related to energy security and waste management. Agricultural wastes, abundantly available worldwide, present a promising alternative to conventional fossil fuels. These wastes can be transformed into valuable products such as methane, hydrogen, biofuels, and various chemicals. This chapter provides a comprehensive exploration of biomass utilization technologies, with a particular emphasis on pyrolysis followed by catalytic steam reforming for hydrogen production. The discussion delves into the application of various metal oxide catalysts used in the steam reforming process, their catalytic performance, and the mechanisms of catalyst deactivation. Additionally, the chapter highlights advanced insights from Density Functional Theory (DFT) studies to deepen the understanding of catalyst behavior and process optimization. Furthermore, the bio-refinery concept is examined to maximize the utilization of by-products, making the process more costeffective and competitive with existing hydrogen production technologies. By integrating these approaches, this chapter underscores the potential of agricultural waste as a sustainable feedstock for hydrogen production, contributing to the global transition toward cleaner energy solutions.
2.	Harnessing machine learning and artificial intelligence for improved thermal operations S Keshri, UN Patil, **K Kumar,** S Singh - Smart Heat Transfer and Thermal Management: Book Chapter, 2026 **Abstract:** Artificial intelligence (AI) and machine learning (ML) optimize the thermal management system and process optimization, revolving changes in the thermal management sector in the application of algorithms and data-driven-based approaches in direct temperature control to different settings. In gas turbines, AI and ML improve the thermal barrier coating through better durability and performance by microstructure analysis and property adjustment. The AI expert systems aid the thermal spray industry by making precise predictions, minimizing error, and reducing costs beyond traditional optimization techniques. Apart from this, it is AI and ML that drive the digital transformation of surface engineering, solving certain defined implementation and optimization challenges. Most importantly, ML is required for the management of heat in electric vehicle batteries through fast charging. In conclusion, AI and ML are at the core of the thermal management advancements because they can create innovative solutions related to efficiency, reliability, and sustainability. This chapter discusses the applications of AI and ML in thermal management and their influence on industries in electronics, automobiles, and manufacturing.
3.	Intelligent visual to textual mapping in automatic medical diagnosis and treatment PS Yadav, DK Tyagi, **SK Vipparthi** - Smart Electronic Devices and Systems for Biomedical and Healthcare Applications: Book Chapter, 2025 **Abstract:** Real-time scene description impacts instant logic for blind or disabled persons. It becomes more critical if related to health. Scene-to-text conversion on biomedical-related images can assist and impel the diagnosis process. Medical image description sorts correct diagnosis and treatment in the right direction, presenting connections in objects that exist in the images useful in clinical findings. Correct findings lead to satisfactory treatment and help early health recovery with time and overall expenditure savings. We have discussed various important approaches and methodologies, together with relevant datasets, applications, limits, future prospects, and finally summarize the application values of biological image description.

4.	Molecular dynamics (MD) **M Moirangthem, K Kumar, SK Meena -** Engineering Nanoparticles for Biomedical Applications: From Theory to Experiment and modelling: Book Chapter, 2026 **Abstract:** Classical molecular dynamics (MD) simulations have been used to investigate the atomistic mechanisms governing the anisotropic growth of gold nanorods in aqueous environments. The influence of surfactants, halide ions, silver ions, seed geometry, and surface polarization is systematically explored to uncover how these parameters modulate facet-specific growth behaviors. The simulations reveal that cetyltrimethylammonium bromide molecules self-assemble into distorted cylindrical micelles on various gold surfaces Au(111), Au(110), and Au(100). These micelles generate water-ion channels that serve as conduits for the diffusion of gold precursor ions (AuCI - 2) toward the gold surface. The Au(111) facet is shown to promote faster growth due to its lower surfactant packing density and higher electrostatic potential difference relative to other facets. The study also examines the differential adsorption behavior of halide ions (CI, Br I), finding that Br and I exhibit stronger surface affinity than CI, thereby influencing micellar structure and nanoparticle morphology. Replacing Br with CI results in less compact surfactant layers, leading to more isotropic growth. Furthermore, the addition of Ag ions enhances surface passivation by increasing Br density and suppressing growth on specific facets. Seed geometry plays a crucial role in directing anisotropy. Penta-twinned seeds display facet-selective micelle adsorption, supporting unidirectional elongation and nanorod formation. Additionally, surface polarization effects are incorporated using virtual electron models to more accurately represent surface interactions. Overall, this study demonstrates how MD simulations can provide mechanistic insights into the growth processes of anisotropic nanoparticles, offering predictive control over shape evolution and contributing to the rational design of nanomaterials with tailored properties.
5.	Nanotechnology in food supply chain management S Akhter, **JA Malik,** SZ Hussain, AM Sofi - Nanotechnology in Food Packaging and Preservation: Book Chapter, 2025 **Abstract:** This chapter offers an in-depth analysis of the application of nanotechnology within the food supply chain, emphasizing its significant influence on food packaging, safety, and quality. It explores the transformative role of various nanomaterials in packaging systems, including active and intelligent solutions such as antimicrobial packaging, gas scavengers, time-temperature indicators, etc. The exploration extends to practical applications of nanotechnology across key stages in the food supply chain, encompassing food production, processing, and packaging. It highlights the limitations of traditional packaging methods and underscores the necessity for advanced techniques to address protection, customization, and sustainability challenges. This chapter investigates the hurdles associated with incorporating nanotechnology into the food industry, focusing on safety concerns, research needs, and regulatory issues. The significance of continued research, responsible implementation, and collaboration is stressed for realizing nanotechnology's vast potential in revolutionizing food safety and ensuring a sustainable future in the food industry.
6.	Reinforcement learning-driven model compression: Structured layer-wise parameter pruning **A Gupta, A Dhamija, M Gupta, P Kukrety, SS Jha, S Mishra**- Frontiers in Artificial Intelligence and Applications: eBook Chapter, 2025 **Abstract:** Deep learning models, albeit having remarkable performance in various image and vision tasks, are notoriously parameter-inefficient. The huge number of parameters in these models makes them unsuitable for large-scale deployment on resource-constrained devices due to high memory and computational requirements. It has also been observed in the literature that many parameters in such deep models are redundant. Hence, there is a need to extract parameter-efficient deep models for wide-scale deployment on resource-constrained devices. To address this challenge, we propose a novel parameter reduction framework using Reinforcement Learning (RL) that performs layer-wise structured pruning of deep models. The proposed method leverages the

	Proximal Policy Optimization (PPO) strategy to assign learnable importance scores to structural units like filters and neurons across all layers of a trained deep model. These scores get sampled from a Bernoulli distribution to determine the pruning decisions. The PPO agents learn using accuracy-aware rewards from a downstream classification task. Additionally, we propose a compression slider mechanism that enables user-defined control over compression rates, ensuring balanced sparsity. Experiments on benchmark models such as VGG16 and AlexNet across two datasets demonstrate that our method achieves better trade-offs between model performance and compression, while offering finer control over pruning granularity. For VGG16 over CIFAR-10, we achieve a total compression of 85.14% with a drop of 2.08% in inference accuracy. Also, for AlexNet, we prune the model by 77.67%, while observing a drop of 2.84% in accuracy. Moreover, our proposed approach enables precise control over the pruning process, allowing for flexible and targeted compression strategies suitable for real-world deployment.
7.	Smart surfaces and coatings: An innovative approach **A Singh,** S Samanta, SK Tiwari - Smart Materials: Biomaterials, Coatings, Energy, Sensors and Structural Engineering: Book Chapter, 2026 **Abstract:** Smart surfaces and coatings have emerged as a significant trend in surface technology in recent time. Their possible applications are varied and hold the promise of transforming numerous industries. These are advanced or intelligent materials that respond dynamically to external stimuli, thereby offering benefits that extend be- yond the fundamental, passive roles of traditional coatings, such as decoration and protection. These stimuli may include heat, light, mechanical forces, temperature changes, pressure variations, pH shifts, and exposure to corrosive ions. As coating technology continues to evolve, these materials have become essential in industrial manufacturing, exhibiting remarkable properties such as superhydrophobicity, self-cleaning capabilities, enhanced antibacterial characteristics, and improved resistance to corrosion. Biomimetics, the study of the structures, functions, and behaviors of liv- ing organisms, has a decisive part in engineering design. The integration of biomi- metic principles with intelligent coating materials can enhance their performance and functionality, foremost to the advancement of even more advanced coatings. In this chapter, various types of intelligent coatings including advanced superhydropho- bic coatings, anticorrosion coatings, and antibacterial coatings are discussed in detail.
B	**Conference Proceeding(s)**
8.	Analysis of multi-material metal laser powder bed fusion process: A semi-analytical approach **A Srivastava, R Kumar, A Agrawal** - International Mechanical Engineering Congress and Exposition, Proceedings (IMECE), 2025 **Abstract:** Among all the metal additive manufacturing processes, the Laser Powder Bed Fusion Process (LPBF) is widely researched for fabricating complex and intricate parts, especially in aerospace, automobile, medical, etc. The process uses a fine raw powder bed that melts and solidifies to fabricate components. Multi-material systems are widely recognized for offering advantages over mono-material systems in various applications; however, their LPBF processing is challenging. The present study has developed a semi-analytical model to study the melt-pool dynamics of multi-material systems, especially metal-metal multi-material systems. The novelty of the formulation lies in incorporating temperature-dependent thermophysical material properties for multi-material systems by employing rule-of-mixture material modelling. The laser heat source is assumed to be a moving two-dimensional Gaussian heat source, which depicts a real-process scenario of LPBF. The Finite volume method has been employed to solve the discretized spatial and temporal domain to estimate the heat loss due to convection and conduction iteratively to obtain the temperature distribution in the powder bed without considering the Marangoni effect, radiative heat loss, and recoil pressure. This model considers the phase change during the melting and the temperature-dependent Thermo-physical properties to get an accurate simulation result. The model analyses the melt pool dynamics along with the molten zone's depth and width dimensions in the laser-material interaction domain with varying process parameters in the LPBF,

	such as laser power, laser scan velocity, etc. The simulation results strongly correlate process parameters and melt pool dimensions at low computational cost. The results concluded that the increasing volume fraction of 10 to 40% for SS304L causes the melt pool depth and width to decrease by approximately 35.71% and 26.32%, respectively.
9.	Black hole search by scattered agents on time-varying dynamic graphs **T Kaur, A Saxena,** PS Mandal, **K Mondal** - International Symposium on Stabilizing, Safety, and Security of Distributed Systems, 2025 **Abstract:** A black hole is a malicious node in a graph that destroys resources entering into it without leaving any trace. The problem of Black Hole Search (BHS) using mobile agents requires that at least one agent survive and terminate after locating the black hole. Recently, this problem is studied on 1-bounded 1-interval connected dynamic graphs, where there is a footprint graph, and at most one edge can disappear from the footprint in a round, provided that the graph remains connected. In this setting, the authors proposed an algorithm that solves the BHS problem when all agents start from a single node (rooted initial configuration). They also proved that at least $2\delta_{BH}+1$ agents are necessary to solve the problem when agents are initially placed arbitrarily across the nodes of the graph (scattered initial configuration), where δ_{BH} denotes the degree of the black hole. In this work, we present an algorithm that solves the BHS problem using $2\delta_{BH}+17$ many initially scattered agents. Our result matches asymptotically with the existing rooted algorithm under the same model assumptions.
10.	Joint sensing and communication for V2V localization using chirp-QPSK waveform in 6G networks **AK Rajak, A Gupta, S Kumar, A Sharma** - IEEE 17th Malaysia International Conference on Communication (MICC), 2025 **Abstract:** The advent of 6 G wireless networks promises seamless integration of sensing and communication functionalities, enabling advanced applications such as Vehicle-to-Vehicle (V2V) localization for Intelligent Transportation Systems (ITS). This paper presents a Joint Sensing and Communication (JSAC) system employing a Chirp-QPSK waveform in the sub- 6 GHz band, implemented using MATLAB Simulations. The system employs the MUSIC algorithm for high-resolution Angle of Arrival (AoA) estimation and FFT-based techniques for range estimation. The simulation demonstrates a range estimation accuracy of 64m, achieving a performance of 98.5%. The proposed system delivers reliable AoA detection and significantly reduces the need for separate radar or GPS modules, ensuring robust operation even in complex multipath environments. Future work will investigate the application of machine learning techniques to Channel State Information (CSI) data to further enhance localization accuracy and robustness under dynamic and non-line-of-sight (NLOS) conditions.
11.	Mechanical properties and small scale fatigue of hybrid (IN718-XH67) additively manufactured nickel based superalloys **RP Chaudhari,** DD Awale, **H Singh,** D Srinivasan, N Jaya Balila - International Mechanical Engineering Congress and Exposition, Proceedings (IMECE), 2025 **Abstract:** This study is a comprehensive evaluation of the microstructure and mechanical properties (tensile and fatigue) of a laser powder bed fusion manufactured novel hybrid system of two nickel-based superalloys, IN718 built on top of XH67. IN718 is a well known γ″ strengthened alloy, while XH67 is a new Nickel based superalloy alloy that has γ′ precipitate strengthening. The objective is to explore the optimum benefits of mechanical properties via additive manufacturing technology, for accelerated alloy development for repair of high temperature materials used in various applications. The microstructure of the stand alone alloy and the hybrid alloy interface was characterized in the as-printed and heat treated condition. The 0.2% yield strength of the as-printed hybrid tended to follow the yield strength of the alloy with the lower strength at room temperature and at 650°C, namely XH67 (~650 MPa), having a ductility in between that of XH67 and IN718 at 35%, whereas after heat treatment, the strength followed the alloy with the higher strength (namely IN718 with ~1000 MPa) at both RT and 650°C. The hybrid failure was seen to take place

	in the alloy with the lower strength (XH67). The fatigue behaviour of the hybrid evaluated at 95% of the yield strength, did not show a significant distinction between the as printed and heat treated conditions at RT, with the cycles to failure lying between 10^4 to 10^5. At 650°C, the hybrid after heat treatment showed a fatigue debit, as compared to the life at room temperature (from 10^5 cycles to 10^3 cycles). The comprehensive study elucidates the possibility of utilizing hybrid alloy systems for potential repair applications.
12.	Microstructure's impact on tool wear during drilling of wrought and WAAM fabricated Ti6Al4V alloy J Singla, **N Kumar,** A Bansal, AK Singla, N Khanna - International Mechanical Engineering Congress and Exposition, Proceedings (IMECE), 2025 **Abstract:** Ti6Al4V alloy's strong strength, low density, and higher corrosion resistance makes it promising for use in a variety of components for automobile and aerospace industries. Wire Arc Additive Manufacturing-Cold Metal Transfer (WAAM-CMT), a contemporary direct energy deposition technology beneath the of additive manufacturing techniques, can be utilized for fabrication of big and complicated parts owing to its properties like high deposition rate, less heat supplied heat input, small spatter, enhanced dimensional performance, and large energy efficiency. Therefore, in this research work, Ti6Al4V alloy was fabricated using WAAM-CMT technique in argon designed chamber in order to avoid oxidation. under designed chamber. Additionally, Additive manufacturing parts typically require post-processing mainly machining to remove surface flaws, making them suitable for industrial application. Therefore, to compare the machinability of conventional and WAAMed Ti6Al4V alloy components, TiN-coated carbide spiral drill bit has been used for drilling under LCO2 environment. Additive manufactured alloy exhibited a distinct microstructure of needle type structure with higher percentage of β grains as compared to conventional one, that showed equiaxial grains with higher percentage of α grains. Tool wear was observed to be greater for drilling of WAAMed Ti6Al4V alloy due to its high hardness and ultimate strength owing to fine structure of α phase in comparison to as-cast material. Tool degradation mechanisms in WAAMed Ti6Al4V alloy were found to have higher adhesion and edge chipping which may be due to higher hardness and enhanced sticking tendency of α and β grains. However, built up edge (BUE) in this case is smaller than that may have been resulted from presence of more β grains. Alternatively, larger BUE and smaller edge chipping were formed during drilling of wrought Ti6Al4V alloy that directly links to the presence of equiaxed grains and less percentage of β grains, respectively.
13.	Optimal dispersion of silent robots in a ring B Das, B Gorain, **K Mondal,** K Mukhopadhyaya, S Pandit - International Symposium on Stabilizing, Safety, and Security of Distributed Systems, 2025 **Abstract:** Given a set of co-located mobile robots in an unknown anonymous graph, the robots must relocate themselves in distinct graph nodes to solve the dispersion problem. In this paper, we consider the dispersion problem for silent robots, i.e., no direct, explicit communication between any two robots. The robots are deployed on the nodes of an oriented n node ring network. They operate in synchronous rounds. The dispersion problem for silent mobile robots has been studied in arbitrary graphs where the robots start from a single source. In this paper, we focus on the dispersion problem for silent mobile robots where robots can start from multiple sources. The robots have unique labels from a range [0,L] for some positive integer L. Any two co-located robots do not have the information about the label of the other robot. The robots have weak multiplicity detection capability, which means they can determine if it is alone on a node. The robots are assumed to be able to identify an increase or decrease in the number of robots present on a node in a particular round. However, the robots can not get the exact number of increase or decrease in the number of robots. We have proposed a deterministic distributed algorithm that solves the dispersion of k robots in an oriented ring in O(logL+k) synchronous rounds with O(logL) bits of memory for each robot. A lower bound Ω(logL+k) on time for the dispersion of k robots on a ring network is presented to establish the optimality of the proposed algorithm.

14.	Reviewing virtual reality's potential in CBRN Training: Synergizing AI, HCI, and psychology for immersive preparedness **RK Rai,** D Kumar, **SS Jha,** RS Kanwar, R Bansal - International Conference on Extended Reality, 2025 **Abstract:** Virtual Reality (VR) technology holds great promise in revolutionizing offline CBRN (Chemical, Biological, Radiological, and Nuclear) training. This research explores the potential of Immersive CBRN training through VR with a primary focus on first responders' insights. First, it assesses the current state of CBRN training, highlighting its strengths and weaknesses. Then, it delves into a survey of first responders, uncovering their needs and expectations regarding VR integration. This includes examining the importance of user-friendly interfaces (HCI), the potential for VR to simulate emotions for enhanced psychological realism, and the role of Artificial Intelligence (AI) in assessing performance and dynamically generating training scenarios. This paper uses survey results and other studies to show how VR can be very useful for training in situations involving CBRN threats. It connects technology with what's actually needed in the real world. Ultimately, it underscores the transformative power of VR technology in making CBRN training safer, immersive and effective, shaping a future of enhanced preparedness.
C	**Article(s)**
15.	1/f noise model for extracting bulk trap density in scaled metal oxide semiconductor field effect transistors **P Khedgarkar,** MD Ganeriwala, **G Gupta, P Duhan** - Journal of Applied Physics, 2025 **Abstract:** 1/*f* noise analysis is a powerful tool for characterizing defects in the bulk of the gate oxide of metal oxide semiconductor field effect transistors (MOSFETs). The bulk trap density (N_{BT}) is often extracted from the commonly used carrier number fluctuation model. This model fits well with thicker gate oxide devices but does not capture the effect of oxide scaling on the 1/*f* noise. As a result, it yields an error of several orders of magnitude in estimating N_{BT} in the scaled devices. In this work, we derive a compact expression of drain current noise power spectral density (S_{ID}) that accurately estimates N_{BT} for scaled devices. Our expression includes terms that account for the position dependence of traps, which is often neglected in previous studies. We validate the robustness of the model by comparing it with the calibrated technology computer-aided design simulations of the advanced 22 nm ultrathin body and buried oxide fully depleted silicon-on-insulator MOSFET device operating in linear, saturation, and subthreshold regions.
16.	A configurable multi input port hybrid inverter topology with quadrupled voltage gain for PV and hybrid applications **BK Gupta, A Kumar, KR Sekhar** - CPSS Transactions on Power Electronics and Applications, 2025 **Abstract:** The presented work demonstrates the three-port inverter configuration for a quadrupled reduction in the operating DC bus voltage compared to conventional inverter topology. Thus, the proposed configuration consists the single inversion stage and operates with single or multiple sources. Irrespective of the source connected at input ports, the three inverters in the tri-inverter configuration synthesize the 512 switching combinations and spread across 61 voltage space locations to realize the load space vector. The switching states are segregated from the space spread not only to realize the maximum voltage gain but also to eliminate the common mode voltage during common DC source operations. In the case of common DC source operation, the CMV eliminated switching combinations ensures the elimination of circulating current with minimum compromise of the voltage gain. The improved voltage gain and eliminated circulating current guarantees the maximum energy yield from source and improved reliability of the converter compared to the conventional inverter. The proposed converter's efficacy and realized space vector switching states in terms of realizable four times voltage gain and the elimination of intra-inverter circulating currents are validated experimentally with single and multiple sources.

17.	ABLE: Attention-based blind learning for universal CSI-free symbol detection **A Ahmad,** A Girdher, C Masouros - IEEE Wireless Communications Letters, 2025 **Abstract:** In this letter, we present an attentive bidirectional long short-term memory (Bi-LSTM)-based symbol estimator, termed ABLE, that directly infers transmitted symbols from received baseband signals without relying on CSI or retraining. ABLE employs a pilot-guided Bi-LSTM Network enhanced with a self-attention mechanism to learn generalized temporal representations and leverages pilot-referenced magnitude and phase information for dynamic adaptation to impairments, such as frequency selectivity, time asynchrony, and dynamic fading conditions. Simulations over a range of wireless channels, including 5G NR-compliant OFDM scenarios, demonstrate that ABLE achieves strong generalization to both seen and unseen conditions, yielding 2-4 dB gains over conventional detection methods.
18.	Access to alkylative/hydrodefluorination of trifluoromethyl ketones using photoexcited dihydropyridines **S Das, D Maity, B Paul, S Patel, I Chatterjee** - Organic Letters, 2025 **Abstract:** A convenient strategy for selective and challenging single C–F bond functionalization of trifluoromethyl ketones has been introduced under visible light irradiation. Photoexcited 1,4-DHP serves a dual purpose as a reductant and a source of alkyl radicals (or H atoms) in the alkylative defluorination and hydrodefluorination processes. The solvent hexafluoroisopropyl alcohol (HFIP) plays a crucial role in the selective single C–F bond cleavage. Overall, a transition-metal- and photocatalyst-free, mild protocol for accessing a broad range of functionalized fluorinated products of high pharmaceutical interest is presented here. Operational simplicity and mechanistic evidence for photoinduced alkyl (or HAT) radical generation highlight the effectiveness of this strategy as a reliable toolbox for selective defluorinative C–C cross-coupling and a hydrodefluorination protocol. 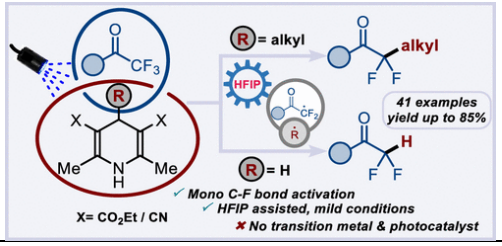
19.	Advanced deep learning techniques for real-time defect detection and quality control in laser cutting processes. P Kumar, **S Rathor** - Lasers in Engineering (Old City Publishing), 2025 **Abstract:** Laser cutting is a high-precision manufacturing technique that relies on the stability of a focused laser beam and an assist gas to produce intricate geometries with minimal mechanical stress. However, fluctuations in beam parameters and gas flow can destabilize the keyhole, leading to defects such as kerf-width deviation, dross attachment, heat-affected zone irregularities, and micro-cracks. Conventional rule-based inspection methods image thresholding and statistical process control suffer from static thresholds and limited adaptability, yielding segmentation accuracies below 85%. This paper presents a comprehensive framework for AI-driven defect detection and quality control in laser cutting. We integrate multi modal in-process sensing (optical, thermal, acoustic) with post-process machine vision, and employ state-of-the-art convolutional neural networks (U-Net, Mask R-CNN) and hybrid CNN–Transformer architectures for pixel-level segmentation and classification of defects. Self- and unsupervised learning strategies reduce annotation overhead by modelling the manifold of "good" cuts and flagging deviations in real time. Our edge-AI implementation achieves inference times under 30 ms, enabling closed-loop feedback to CNC controllers that adjust process parameters on the fly. Benchmarking on publicly available metal surface datasets demonstrates detection accuracies > 95%, Intersection over Union scores > 0.80, and F1-scores > 0.90. We further analyse the hardware and software requirements for industrial deployment, quantify the cost–benefit, and address integration challenges with

	MES/SCADA systems. Finally, we outline future directions miniaturized edge-AI modules, Deep Learning based AI diagnostics, and digital-twin coupling to realize zero-defect, self-optimizing laser-cutting cells in smart factories.
20.	An efficient method for site-selective boronation of peptides and proteins applied in magnified bacterial imaging **S Chatterjee, A Chowdhury, N Verma,** S Basa, **NM Tripathi, V Gour,** V Rai, **A Bandyopadhyay** - Nature Communications, 2025 **Abstract:** Borylated compounds have received tremendous attention in chemical biology and drug design. Motivated by this notion, we develop an efficient methodology for boron incorporation into peptides and proteins via chemoselective conjugation of cysteine residues under catalyst-, additive-, and metal-free conditions. By harnessing the optimum S_N2 displacement profile of bromomethyl boronate, we establish a methodology that enables the selective incorporation of methylboronic acid into various peptides, including bioactive constructs, as well as proteins with rapid kinetics ($>10^2$ $M^{-1}s^{-1}$) and excellent conversions at physiological pH. The method also leverages rapid access to bivalent boron conjugates, which, when applied to clinically used antimicrobial peptide UBI(29-41), augment its binding efficacy (40-fold) via covalent capture of the diols on bacterial surface glycans, mainly wall teichoic acid (and thus lipoteichoic acid). Notably, bis-boronated UBI exhibits selective staining of *S. aureus* over gram-negative bacteria and mammalian cells, alongside a 14-fold increase in serum half-life compared to native UBI.
21.	An investigation on volumetric absorption system for solar thermal energy conversion and storage **AS Kashyap,** V Bhalla, **H Tyagi** - Thermal Science and Engineering Progress, 2025 **Abstract:** Solar energy offers a promising alternative to fossil fuels for various domestic and industrial thermal applications. Compared to surface absorption-based conventional flat plate collectors, volumetric absorption in nanofluids has been marked as a great technology providing enhanced thermal efficiency. The present study focuses on the volumetric absorption within amorphous carbon-based nanofluid at stagnant conditions in a metallic (copper-based) volumetric receiver. To obtain the optimized thermal performance, the detailed experiments using various mass fractions (10 mg/l, 20 mg/l, 30 mg/l, 40 mg/l, and 50 mg/l) of amorphous carbon-based nanofluid are conducted. In addition, the receiver's surface temperature is measured. The maximum average temperature rise above ambient is obtained for 40 mg/l mass fraction, and the value is 36.1 °C for the nanofluid and 33.9 °C for the surface of the receiver. Through the present study, the authors explore the possibility of integrating a volumetric absorption-based solar collectors (VAS) directly with the phase change material (PCM) for thermal energy storage (TES). Based on the experimental results on VAS, a computational study is conducted where the metallic (copper-based) volumetric receiver is integrated with PCM (RT31). From the computational investigation, it is obtained that the temperature of the PCM increases with increases in the nanofluid's temperature. After heating for 5 min, the average temperature of the nanofluid reaches 51.7 °C; correspondingly for PCM, the temperature reaches 30.7 °C with a liquid fraction of 0.36. Graphical Abstract 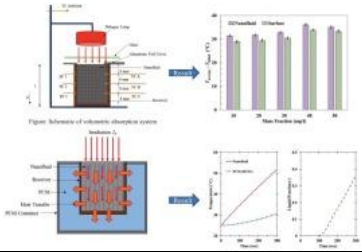
22.	Analytical solution for inverse estimation of groundwater recharge from transient thermal response in stratified media **V Bashist, R Sarmah, I Sonkar** - Journal of Hydrologic Engineering, 2026 **Abstract:** Understanding transient heat transport in a layered subsurface media is essential for applications ranging from groundwater recharge estimation to climate signal detection in soil. This

	study presents an analytical model for 1D transient heat transfer in an N-layered soil system, accounting for realistic surface temperature variations induced by diurnal, seasonal, and long-term climatic trends. The governing advection-conduction equation is solved using the generalized integral transform technique, which inherently enforces interfacial continuity of temperature and heat flux across soil layers without the need for recursive matching or numerical Laplace inversion. The proposed solution is validated against existing analytical and numerical models, demonstrating excellent agreement in homogeneous and stratified domains. A local sensitivity analysis identifies key hydrothermal parameters influencing subsurface temperature behavior. The model's inverse capability is further demonstrated through integration with a genetic algorithm, enabling the estimation of vertical water flux from synthetic temperature-depth data and observed field measurements. This work provides the first fully analytical, scalable, and computationally efficient framework for simulating and interpreting subsurface temperature dynamics in stratified systems. Its flexibility and robustness also make it readily applicable to other diffusion-driven transport processes, such as solute and vapor migration in layered geological formations, thereby enhancing its interdisciplinary relevance.
23.	Azo-based Schiff base as a turn-off fluorescent sensor for Fe3+ and its photophysical study A Kuwar… **N Singh,** R Bendre - Inorganic Chemistry Communications, 2025 **Abstract:** A novel azo dye–based Schiff base receptors **1** and **2** were designed and synthesized via a sequence of steps and characterized by ^{1}H NMR and single crystal X-ray crystallography. The cation recognition properties of receptor **2** were systematically investigated using fluorescence spectroscopy. Notably, receptor **2** displayed a distinct "turn-off" fluorescence response that was highly selective towards Fe^{3+} ions, with no significant interference from other tested cations. The binding studies revealed a detection limit as low as 2.5 μM, demonstrating the high sensitivity of receptor **2**. Furthermore, the practical applicability of receptor **2** was validated by successfully determining Fe^{3+} levels in a pharmaceutical drug sample. These findings highlight the design synthesis of new receptor **2** as a promising, cost-effective fluorescent receptor for the selective detection of Fe^{3+} ions. 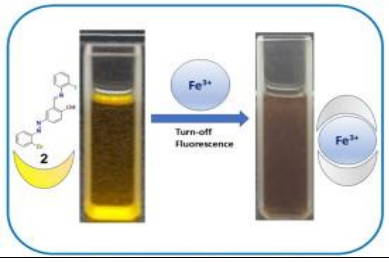
24.	Boundary Carroll CFTs: SUSY and superstrings A Bagchi, **S Chakrabortty, P Chakraborty, R Chatterjee,** P Pandit - Journal of High Energy Physics, 2025 **Abstract:** We consider two dimensional superconformal Carrollian theories with boundaries and construct two variants of the Boundary Superconformal Carrollian Algebra (BSCCA), viz. the Homogeneous and the Inhomogeneous, by making appropriate identification of the parent superconformal Carrollian algebras. These new algebras are then recovered by appropriate limits of a single copy of Super Virasoro algebra. We then focus on the theory of null tensionless superstrings and construct, for the first time, an open null superstring. The Homogeneous version of the BSCCA is realised as worldsheet symmetries on this open null superstring.
25.	Caught in the scroll: Emotion regulation, escapism, and conscientiousness in short-form video use–related disruptions **P Singh, D Kumari, D Sahu** - Social Science Computer Review, 2025 **Abstract:** Emerging social media platforms have become integral to daily life by fulfilling users' needs for information, expression, and social connection. Short-form videos (SFVs) are especially popular among youth due to their personalized and immersive design. Research has highlighted that, in educational settings, social media–assisted instructional approaches can enhance

	motivation, participation, and performance; however, the abundance of non-educational content on SFV platforms may hinder students' self-regulation and academic focus. Excessive engagement may impair concentration, increase procrastination, reduce classroom participation, and heighten stress, anxiety, and depression. Despite growing concerns on excessive SFV usage, limited attention has been given to how such consumption disrupts students' daily functioning and the psychological mechanisms involved. Addressing this gap, the present study examines escapism as a mediator between emotion regulation difficulties (ERDs) and SFV-related functioning disruptions, and investigates conscientiousness as a moderating factor in this relationship. Data was collected from B.Tech students (N = 303) enrolled in technical institutions across India through an online survey using standardized measures. Collected data was subjected to regression, mediation and moderation analysis using SPSS v.30 and PROCESS macro. It was found that escapism was a significant mediator in the relationship of ERDs and interference from SFV consumption and conscientiousness emerged as a moderator of the relationship between ERDs and escapism. The study provides deeper theoretical insights into the psychological drivers of SFV-related dysfunction and informs strategies for mitigating its negative academic and psychological impacts. The results can aid in designing digital well-being interventions, guiding educators and parents in fostering responsible SFV consumption among students.
26.	Cu(I)-anchored NHC-functionalized covalent organic framework (COF) for catalyzing CO_2 chemical fixation into high-value compounds **V Parihar, P Rani, S Kumar, P Beniwal, CM Nagaraja** - Inorganic Chemistry, 2025 **Abstract:** Rapid urbanization has intensified global energy demands, leading to elevated carbon dioxide emissions. Therefore, capturing and utilizing CO_2 as a C1 feedstock is a viable way to synthesize value-added compounds while mitigating carbon emissions. Consequently, this study reveals the sensible design of an effective and highly reusable catalyst for efficiently exploiting CO_2 for the production of useful chemicals. For this, we designed an imidazole-based ionic COF (IL-COF), which was utilized to anchor eco-friendly alkynophilic, non-noble, Cu(I) metal ions to get an NHC (N-heterocyclic-carbene)-based covalent organic framework (COF), Cu(I)-NHC-COF. The catalyst showed outstanding performance for the transformation of CO_2 with propargylic alcohols to produce α-alkylidene cyclic carbonates (α-ACCs) and further promoted a one-pot, 3-component reaction of secondary amines and propargylic alcohols to obtain highly valuable β-oxopropylcarbamates. Additionally, the comprehensive theoretical investigations revealed the detailed reaction pathways for CO_2 coupling leading to the synthesis of α-ACCs and β-oxopropylcarbamates catalyzed by Cu(I)-NHC-COF. Moreover, NHC-COF presented excellent recyclability for several catalytic cycles without potential leaching and retained its chemical stability and catalytic activity. Overall, this study showcases a sustainable and green methodology of utilizing a noble-metal-free COF for the exploitation of CO_2 into high value carbamates and carbonates under ambient conditions. 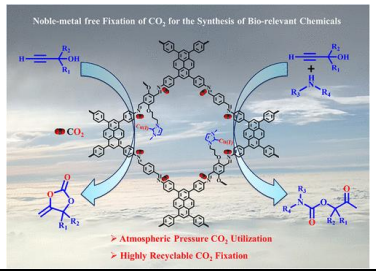
27.	Developing resilient hydrogen transportation networks: Economic and demand-based insights from an Indian perspective **S Sharma, AH Sahir** - International Journal of Hydrogen Energy, 2026 **Abstract:** Hydrogen transmission pipelines are expected to play a significant role in enabling large-scale hydrogen deployment. This study presents a comprehensive analysis of hydrogen transmission pipelines, focusing on the interplay between pipeline diameter, compressor placement, distance, and demand in determining the Levelized Cost of Hydrogen (LCOH) solely

	associated with transportation. Two case studies are evaluated: a fixed compressor placement scenario across 300 km, and a demand-constrained system with adaptive compressor placement under 600–1000 tons of H_2 per day throughput. Results demonstrate that small undersized pipelines lead to disproportionately high operating costs, while oversizing can incur excessive capital expenditure at low demand. Optimal diameters vary with distance and throughput, with 36–48″ preferred for long-distance fixed-spacing systems, and 18–22″ providing resilience under constrained demand scenario. The analysis shows that achieving cost-competitive hydrogen transport in India requires balancing pipeline diameter with demand forecasts, to accelerate infrastructure rollout. Policy analysis highlights India's emerging regulatory landscape, emphasizing the need for harmonized safety standards, and demand-aligned infrastructure planning. 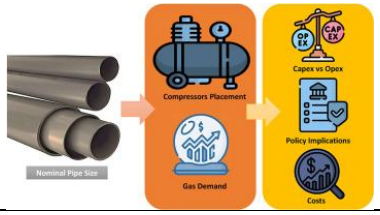
28.	Direct numerical simulation of ionic transport of non-Newtonian electrolytes through patterned surface **S Maurya,** M Trivedi, **N Nirmalkar** - Physics of Fluids, 2025 **Abstract:** The transport of electrolytes and ions across ion-selective interfaces form the basis of modern electrochemical and separation technologies, including energy storage, desalination, electrochemical sensing, and microfluidic separation. While ion migration and flow dynamics in Newtonian electrolytes have been widely explored, the role of non-Newtonian rheology, particularly shear-thinning behavior, on electrokinetic transport and instabilities remains not fully understood. In this study, ion transport across patterned ion-selective membranes is investigated using numerical simulations. The coupled Poisson–Nernst–Planck and Navier–Stokes equations are solved to capture electrostatic potential, ionic migration, and fluid flow under shear-dependent viscosity. Results reveal that shear-thinning electrolytes destabilize otherwise uniform electroosmotic convection producing chaotic flow structures and variable current responses through the membrane. This destabilization lowers the threshold for the onset of convective instabilities, thereby enhancing chaotic convective mixing and promoting spatially uniform ion distributions, which elevate overlimiting currents. Moreover, shear-thinning behavior sharpens velocity and concentration gradients near the membrane surface, leading to improved ionic flux. Patterned membrane geometries further regulate ion transport by modifying electroosmotic fields and reducing permeable surface areas, thereby amplifying overall transport efficiency. Collectively, the coupling between electrolyte rheology and patterned membrane distributions enable enhanced and controllable ionic transport dynamics. These insights address critical challenges such as mitigating dendrite formation in electrochemical systems, improving operational lifetimes, and guiding the development of advanced membrane architectures. Flow and concentration fields are interpreted through ionic concentration, velocity distributions, integrated mixing efficiency, and spatial–temporal variations of ionic current densities.
29.	Do socio-political factors impact terrorism? Insights from Jammu and Kashmir in India **NK Soni, P Singh** - Deviant Behavior, 2025 **Abstract:** Terrorism is often linked to socio-political and demographic factors, but scientific literature remains divided on their significance. The present study explores whether such factors significantly associate with terrorism in the Indian context. This study explores association of social (rural-urban population, houseless population, literacy), political (governance, administrative divisions), ideological, demographic (population density, geopolitical distance from border, rural-urban male), economic (persons below poverty line, marginal land holdings, backward population, main occupations), and religious factors with terrorism in Jammu &

	Kashmir. Results revealed no significant relationship between the selected factors and terrorism, suggesting that deeper, localized drivers of terrorism are at play.
30.	ELIGANT-TN–ELI Gamma above neutron threshold: The thermal neutron setup PA Söderström… **D Choudhury**… **R Roy**… GV Turturica - Nuclear Instruments and Methods in Physics Research Section A: Accelerators, Spectrometers, Detectors and Associated Equipment, 2025 **Abstract:** Here we present the thermal neutron counter from the ELI Gamma Above Neutron Threshold setup at the Extreme Light Infrastructure – Nuclear Physics. We describe the mechanical design of the setup, the properties of the ^{3}He gas counters, and the hardware data-acquisition electronics and software digital signal processing. The performance of the complete detector array is demonstrated via Geant4 and MCNP simulations, and measurements with typical neutron sources. The analysis procedure for experimental measurements are outlined with a in-beam test experiment with an α beam to measure the $^{13}C(\alpha,n_0)^{16}O$ cross-section branching ratios.
31.	Energy-efficient gas sensing of NO and NO_2 at room temperature using poly(triarylamine) organic semiconductor A Chaurasiya, **AK Singh,** D Panda - IEEE Sensors Journal, 2025 **Abstract:** NO_2 and NO are among the most hazardous environmental gases, primarily generated from fossil fuel combustion, and power plants, posing a serious challenge for achieving Sustainable Development Goals (SDG 3). Poly(triarylamine) (PTAA), a polymer with a delocalized π-conjugated backbone has been investigated for its efficacy in gas sensing under ambient conditions. Herein, a PTAA thin-film semiconductor gas sensor is fabricated and systematically evaluated for the detection of nitrogen dioxide (NO_2) and nitric oxide (NO) at room temperature. Thin films of PTAA are deposited onto prefabricated interdigitated electrodes (IDEs) by drop-drying a solution of PTAA in chloroform, ensuring straightforward device integration. The structural and morphological features of PTAA are characterized by using spectro-microscopic techniques. The fabricated sensors exhibit clear and reproducible responses of 70.8% and 27.8% toward 5 ppm NO_2 and NO, respectively, supported by repeatability, response, and recovery characteristics. In addition, the PTAA sensor showed the highest NO_2 selectivity when tested against common exhaust pollutants (H_2S, SO_2, NH_3). The response and recovery times toward NO_2 were recorded as 295 s and 505 s, respectively, highlighting superior sensitivity and faster recovery dynamics when compared to NO. These findings establish PTAA as a promising organic semiconductor for the selective detection of NOx gases.
32.	Enhancing aromatic selectivity via non-conventionally modified Mo/MCM-22 catalyst in a nonoxidative methane dehydroaromatization reaction AC Kothari, **S Bhandari,** S Singh, P Lama, R Bal - Topics in Catalysis, 2025 **Abstract:** The direct catalytic conversion of methane to higher aliphatic/aromatic hydrocarbons is a key challenge due to coking at high temperatures, which decreases the stability of the catalyst. This study investigates the synthesis of new Mo-modified MCM-22 catalysts for methane dehydroaromatization (MDA) reaction where the controlled dispersion of metal on aluminosilicate supports plays a crucial role. Molybdenum (Mo) was successfully incorporated into MCM-22 in various amounts (3–7 wt%) via thermal decomposition of prepared molybdenum precursor in a non-conventional method, and characterisation was done using XRD, FTIR, SEM, BET, NMR, NH_3-TPD, H_2-TPR and TEM. TEM images of the 5% Mo-loaded catalyst revealed an average particle size of 2 nm. NH_3-TPD studies indicated the improvement of the moderate acidic character of the catalyst. Solid-state NMR studies demonstrated strong Mo-zeolite lattice interactions, where Brønsted acid sites facilitate Mo migration and anchoring through oxygen bridges to framework aluminium. Excess molybdenum incorporation leads to greater interaction with the support, leading to aluminium expulsion, forming non-framework species and $Al_2(MoO_4)_3$, indicating that the control molybdenum addition is essential for the host framework to retain structural integrity. Moreover, the synergistic effects between Mo and Brønsted acid sites provided superior catalytic performance at 5 wt% Mo loading (5Mo/MCM-22) with methane conversion of ~ 11.6% and

	benzene selectivity of ~ 87% at 700 °C. This study highlights the significance of Mo loading on MCM-22 for improved benzene selectivity in methane dehydroaromatization reaction. 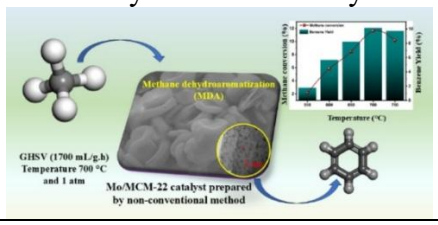
33.	Experimental study of sustainable bioenergy generation from woody and agricultural residue using a downdraft fixed-bed gasifier **SA Waziri, I Dhada, R Das,** AK Shukla - Energy Reports, 2025 **Abstract:** The surging need for sustainable clean energy has accelerated the shift toward carbon-neutral fuels. Gasification offers an effective route for harnessing biomass energy potential, significantly enhancing its utility through conversion into a combustible fuel gas. This study evaluated the performance and efficiency of four North Indian feedstocks using a 10-kW downdraft gasifier. The feedstocks are eucalyptus *(Eucalyptus globulus),* poplar *(Populus ciliata),* bagasse *(Gramineae Saccharum officinarum),* and coconut shell *(Cocos nucifera).* The study assessed syngas composition, equivalence ratio (ER), calorific value (CV), carbon conversion efficiency (CCE), and cold gas efficiency (CGE). Moreover, Potential CO_2 mitigation (PCO_2M), energy density (ED), fossil fuel equivalent (FFE), fuel ratio (FR) and thermal stability (TS) have been evaluated. The results indicate that the average CV of poplar is 5.911 $MJ.m^{-3}$, eucalyptus is 5.246 $MJ.m^{-3}$, coconut shell is 6.162 $MJ.m^{-3}$, and bagasse is 4.248 $MJ.m^{-3}$. The CGE indicated optimum efficiencies of 49.51 %, 51.34 %, 48.60 %, and 32.44 % for poplar, eucalyptus, coconut shell, and sugarcane bagasse, respectively. The CCE also demonstrated remarkable conversion rates. The energy density noted was highest for coconut shell at 11.319 GJ/m^3, and lowest for bagasse at 4.977 GJ/m^3. The potential CO_2 mitigation concerning petroleum is 1048.59 kg of CO_2/m^3 of biomass for coconut shell, 916.69 kg of CO_2/m^3 for poplar, 885.00 kg of CO_2/m^3 for eucalyptus, and 461.07 kg of CO_2/m^3 for bagasse. This study offers a comparative insight with published literature, revealing the strong potential of the examined feedstocks for efficient energy generation, especially in rural areas where their untapped availability often leads to environmentally harmful disposal.
34.	Exploring remote C─ H bond arylation: Transition metal catalysis without “End-On Template” **B Paul, I Chatterjee** - Helvetica Chimica Acta, 2025 **Abstract:** C─H bond functionalization has appeared as one of the most efficient tools for building complex molecular scaffolds. Despite growing interest in remote C─H bond functionalization, achieving the distal site selectivity is highly challenging. Traditional *“end-on template”* based methods usually require additional steps for installing and removing long directing templates, and often rely on expensive transition metals, which makes the process less sustainable. In this essay, an alternative concept known as *“complementary catalysis”* is discussed to achieve remote C─H arylation without the use of large templates. This approach requires a small directing group to control regioselectivity under mild conditions without any externally added ligands or activators. Most importantly, it paves a more sustainable route by improving the atom and step economy.
35.	First-principles investigation of surface functionalization in double-transition-metal ScYX (X= C, N) MXenes **A Pandey, N Sardana** - Computational Condensed Matter, 2025 **Abstract:** The exfoliation of certain MAX phase solids into two-dimensional layered materials known as MXenes. This article investigates the geometrical properties, dynamical stability, mechanical properties, electronic properties with both GGA and HSE06, work function, and optical characteristics of the single-layer pristine 1T-ScYX (X = C/N) MXenes, as well as functionalized 1T-$ScYXZ_2$ MXenes with surface termination group OH, S, Se, F, Cl, Br, and I (iodine) via VASP. The results of this study illustrate that surface functionalization strongly alter

	the vibrational, mechanical, electronic, and optical properties of pristine ScYX MXenes. In addition, functionalization enhances its mechanical characteristics. Moreover, functionalization alters the metallic properties of ScYC MXenes, while ScYN MXenes maintain their metallic characteristics after functionalization. $ScYCO_2$ demonstrated the largest band gap of 1.83 eV (GGA) and 2.98 eV (HSE06). ScYC and ScYN signify the negative values of real part of dielectric function in the near-infrared spectrum, highlighting their appropriateness for plasmonic applications owing to their minimal imaginary component. The peak energy loss function value for $ScYXZ_2$ MXenes was observed between 7 and 20 eV, whereas for pristine MXenes ScYC and ScYN, it was noted within the 15 eV range. $ScYCZ_2$ semiconductor MXenes, possessing a higher Poisson ratio, could be employed in flexible electronic and optical materials. 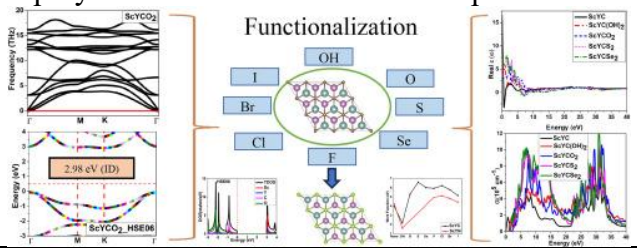
36.	Government strategies to economically support the cleaning of water bodies in India A Gani, A Hussain, **S Pathak** - Wastewater to Resource Recovery: Applying the Circular Economy Towards Sustainable Development, 2025 **Abstract:** This chapter examines the various approaches undertaken by the Indian government to provide financial support for the nationwide cleanup of water bodies. It explores the programs, resources, and policies intended to address the worldwide issue of water pollution, which poses significant environmental and public health hazards. The chapter also provides an overview of the current condition of India's water bodies, identifying the main contaminants and their sources. The changes in government interventions over time, from earlier rules and regulations to modern integrated approaches, have also been discussed. The study includes significant national initiatives that demonstrate the government's dedication to preserving and restoring clean water bodies, such as the Swachh Bharat Abhiyan, the National River Conservation Plan, and the Ganga Action Plan. A comprehensive review is conducted on the economic support mechanisms, which encompass the creation of pollution control boards, public financial allotments, and the application of the polluter pays concept. The chapter delves into novel financing mechanisms that sustainably support water-cleaning initiatives, including international funding, green bonds, and public–private partnerships. Along with adopting eco-friendly practices and infrastructure, the chapter also emphasizes the use of technology and data analytics in the monitoring and management of water quality. The chapter concludes with a thorough examination of the achievements and difficulties associated with the Indian government's economic approaches used for water body cleansing. It makes policy proposals to improve the strategies that are now in place, highlighting the necessity of integrated and sustainable economic models to guarantee the long-term preservation and cleanliness of India's essential water resources.
37.	Homogenization of boundary optimal control problem governed by heat equation in domain with rugose boundary **R Raj** - Asymptotic Analysis, 2025 **Abstract:** In this article, we investigate the boundary optimal control problem associated with Heat equation in a two-dimensional highly oscillating domain $\Omega\epsilon$ in which the control is applied periodically via Neumann condition on the oscillating part of the boundary. We characterize the optimal control in terms of unfolding operator and then study the homogenization to obtain two limit optimal control problems depending on the scalar parameters. In the limit optimal control problem, we obtain three controls, namely interior control, an interfacial control and a boundary control.
38.	Imine linked CuII-metallopolymer: A sustainable Electrocatalyst for hydrogen production N Kumar… **K Satpute**… TK Ghorai - Inorganic Chemistry Communications, 2025

	Abstract: Despite extensive efforts, only limited breakthroughs have been made in developing low-cost, efficient, and durable electrocatalysts. In this context, coordination polymers have emerged as promising sustainable catalysts, offering low overpotentials and high durability for electrocatalytic applications related to energy and environmental challenges. In this work, a parqueted two-dimensional (2D) polymeric chain, $[\mathbf{C_{18}H_{16}CuF_2N_2O_2}]_n$ (Cu-polymer), has been constructed by using fluorinated Schiff base [*N,N′*-bis (5-fluoro-salicylidene)-butanediamine] (H_2L) ligand by a facile, simple, slow evaporation route. Its formation is validated by UV, FTIR, and single-crystal X-ray diffraction (SCXRD). Cu-polymer crystallizes in a monoclinic system with the C2/c space group, forming polymeric chains composed of alternating Cu_2O_2 and $Cu_2N_4C_8$ rectangular grid layers. XPS analyses show that the Cu center is in +2 oxidation state. TGA outcomes indicate that the Cu-polymer is thermally stable up to ~317 °C. Cu-polymer displays better HER performance, achieving a current density of 10 mA cm^{-2} at an overpotential of 528 mV with a low Tafel slope of 267 mV dec^{-1} in 0.25 M acetate buffer. It exhibits a high electrochemically active surface area (0.35 cm^2), low charge-transfer resistance, and a turnover frequency of 2.17 s^{-1} per Cu site at 550 mV overpotential. Additionally, the catalyst shows strong durability, maintaining its activity over 12 h with only a 5.3 % loss in current density, highlighting its robustness for hydrogen production. 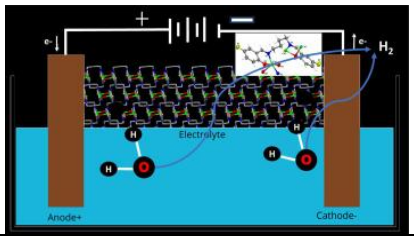
39.	Impact of input wavelength and fiber numerical aperture on multimode soliton dynamics in GRIN-MMFs **LK Sharma, V Pal** - Optics Communications, 2025 **Abstract:** Optical solitons propagating through a multimode fiber (MMF) exhibit peculiar properties in terms of their pulsewidths and characteristic spectral red-shift, offering potential for a wide range of practical applications. In this work, we numerically investigate the dependence of such peculiar properties of femtosecond spatiotemporal solitons in a parabolic graded-index multimode fiber (GRIN-MMF) on the wavelength of the input pulse and on the numerical aperture (NA) of a MMF. Our findings reveal that, at intermediate values of input energies - between the purely linear propagation and multimode (MM) soliton regime - the field exhibits a quasi-MM solitonic behavior. In this transition region, inter-modal four-wave mixing (IM-FWM) transiently redistributes energy among modes, driving a net flow of energy from higher to lower-order modes. With increasing input energy, Kerr and Raman-induced energy transfer accelerate this process, ultimately concentrating most of the energy into the fundamental mode. We also observed that the characteristic MM soliton energy increases with the increase in wavelength of the input pulse, whereas a higher NA of the MMF reduces the MM soliton energy and enhances the Raman-induced soliton self-frequency shifting (SSFS). We also compared our numerically obtained value of MM soliton wavelengths with the theory of SSFS, and a reasonably good agreement was found over a limited range of input pulse energy. Our findings concerning the spatiotemporal solitons in GRIN-MMFs may deepen our understanding and improve control of complex nonlinear wave dynamics in multimode platforms, and in applications involving MM solitons in GRIN-MMFs, particularly when specific soliton properties are desired.
40.	Inducing in situ delamination monitoring with enhanced fracture toughness in fiber‐metal laminates using carbon nanotubes **V Kumar,** N Gupta, **PK Agnihotri** - Polymer Composites, 2025 **Abstract:** Timely and accurate sensing of delamination/damage and improving the fracture toughness of fiber metal laminates (FMLs) is important to ensure their structural integrity in

	advanced applications. Here, we demonstrate an efficient strategy to simultaneously improve the fracture toughness and induce in situ damage sensing capabilities in FMLs using carbon nanotubes (CNTs). Experimental results show that CNT addition improves the flexural modulus (19%), mode-I (36%), and mode-II (64%) fracture toughness of FMLs. Fractography analysis reveals additional fracture mechanisms after CNT dispersion in conventional FMLs. Higher roughness of the composite layer, CNT pullout, and formation of epoxy cusp are primarily responsible for enhanced fracture toughness in FMLC. In addition, the CNTs form a conducting path within the epoxy and improve the electrical conductivity of FMLs by 3–4 orders of magnitude. This enables in situ delamination/damage sensing in FMLC by monitoring the relative change in their electrical resistance (%R). The variation in %R is able to capture damage accumulation as well as stable and unstable growth of delamination cracks. Thus, CNT modification offers dual advantages of improving the fracture properties and inducing in situ damage sensing capability in conventional FMLs.
41.	Influence of a finite step on oblique scattering by a plane vertical barrier **D Goyal, SC Martha,** BN Mandal - Quarterly Journal of Mechanics and Applied Mathematics, 2025 **Abstract:** The problem of water wave scattering by partially immersed thin vertical barrier with two distinct geometrical configurations in the presence of a finite step is examined. For each barrier configuration, the problem is reduced to solving an integral equation or a coupled first-kind integral equations that involve the horizontal component of velocity across the gap below the barrier and above the finite step. The integral equations are solved employing the Galerkin approximation, which involves expansion in terms of product of simple polynomials and exponential decay function multiplied by suitable weight functions whose form is dictated by the edge condition at the submerged ends of the barrier and the edge of the step. Very accurate numerical estimates for reflection and transmission coefficients are obtained and depicted graphically against the angle of incidence for the fixed wavenumbers and against wavenumbers for fixed angle of incidence. The study found that there exists a critical angle for fixed wavenumbers for both configurations at which reflection is minimum and transmission is maximum. The increase in depth ratio plays significant role in decreasing the reflection coefficient for both configurations. For lower frequencies, Configuration I has more reflection while for higher frequencies configuration II has more reflection. The wave force on the barrier has been evaluated for both configurations, and it is observed that the force is higher in Configuration II when the wave propagates from the lower depth region to the higher depth region. Furthermore, the free-surface depression has been plotted for both configurations, illustrating the distribution of wave energy across the respective regions.
42.	Influence of pulsed laser on bead morphology of stainless steel 316L micro-wire in directed energy deposition **S Rathor, R Kant, E Singla,** P Kumar - Lasers in Engineering (Old City Publishing), 2025 **Abstract:** Directed energy deposition (DED) with wire as the deposited material has shown great potential for additive manufacturing of thin-wall geometry. It offers higher material deposition efficiency, minimal material wastage, and a cleaner process environment using wire as a feed material. Micro-wires' use got less attention to understanding the manufacturing of high aspect ratio beads, primarily by increasing the height compared to width. So, this study aims to investigate the single-layer deposited samples of stainless steel 316L micro-wire. Processing conditions for continuous wave (CW) and pulsed wave (PW) laser emission investigated for single-layer deposition regarding surface roughness, bead geometry, microstructure, and microhardness. The single layer deposition with an aspect ratio up to 1 was produced successfully, where layer height was between 0.6 and 0.7 mm. The results show that using micro-wire and PW laser yields lower heat affected zone (HAZ) close to powder-bed additive manufacturing (AM) processes.
43.	Influence of shear-thinning rheology on electroconvection around ion-selective membrane **S Maurya,** M Trivedi, **N Nirmalkar** - Journal of Non-Newtonian Fluid Mechanics, 2025

	Abstract: In recent years, ion-selective membranes and membrane-based separation technologies have garnered significant attention due to their increasing integration in various industries, including energy storage and electrolyzer applications, which enable chemical extraction and/or separation via relevant phenomena such as electrodialysis, desalination, flow electrodes, capacitive deionization, and redox-flow battery systems. The interaction between the membrane surface and the electro-rheological (ER) properties of fluid modulates the inherent ion transport dynamics. The induced electric current subsequently alters the flow field, thereby either enhancing or inhibiting the overall separation efficiency, depending on the applied electric field strength. Additionally, given the non-uniform ionic concentration distribution near the membrane surface, electro-convective currents ultimately lead to a net over-limiting current, followed by a relative suppression of advective ion transport. Such irregular loading and unloading cycles may lead to excessive ion accumulation on electrode surfaces, accelerating dendrite formation, which in turn degrades electrode performance and compromises membrane integrity. Therefore, the present study investigates the role of shear-thinning electrolytes in mitigating electroconvection near ion-selective membranes. A computational model is employed to solve the coupled Poisson-Nernst–Planck equation and the momentum equations, which leads to the evolution of ion distribution profiles and electrokinetic flow instabilities. The extensive numerical simulations yielded the flow attributes in terms of instantaneous velocity, concentration contours, streamlines, ionic current density, and average kinetic energy. In contrast, prolonged chaotic convection facilitates a more uniform distribution of ions within the electrolyte. The enhanced shear thinning effect sharpens both velocity and ionic concentration gradients adjacent to the membrane surface, thereby increasing ionic flux. In general, shear-thinning electrolytes present a promising strategy for mitigating dendrite formation, ultimately improving the operational stability and longevity of electrochemical devices. 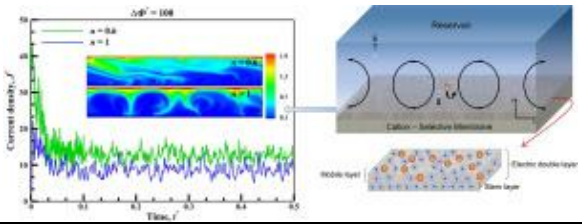
44.	Innovative approach to detect wormhole attack from vehicular ad-hoc network by using variable control chart S Ali, P Nand, S Tiwari, **K Hemlata** - International Journal of Vehicle Information and Communication Systems, 2026 **Abstract:** The wireless nature of Vehicular Ad-hoc Network (VANET) has made it more sensitive towards various types of attacks. Wormhole is one of the attacks by which the security of VANET's routing may be disturbed. In this research paper an innovative approach based on variable control chart is proposed to detect the wormhole attack from VANET. Variable control chart is used in industry to judge the quality of predefined process. This approach can detect misbehaving (i.e., wormhole, black hole) nodes in real time by applying the monitoring system at every receiving node within the network. Here, SUMO 0.32.0 and NS-2.35 simulators are used. The results signify that the proposed approach is capable to detect the wormhole attack on VANET. The novelty of this research work is that a new approach based on variable control chart is used to make the VANET more secure by detecting the wormhole attack on VANET. Copyright
45.	Integrating vision and language: a novel approach to translation for low-resource Indic languages **S Chauhan**, S Saxena, **S Jain** - Asia Pacific Translation and Intercultural Studies, 2025 **Abstract:** Cross-lingual learning provides an excellent chance for knowledge transfer across multiple languages. However, the substantial resource disparity between high- and low-resource languages creates considerable issues. This study focuses on two Indic language families, Indo-Aryan, and Dravidian, as well as a definitely endangered low-resource language that often lacks the extensive training data available in high-resource languages, such as English. We present a unique approach termed Resource-Aware Multimodal Translation (RAMT), which combines large

	language models with vision-based character recognition to improve translation efficacy across a range of resource levels. RAMT uses the Continuous Wavelet Transform to translate low-resource text into a spatial representation, enabling a plug-and-play training process. This method streamlines the training process across multiple languages, reducing reliance on large datasets and enhancing model portability. In addition, our method captures sequential dependencies and spatial properties in the text, which improves stroke extraction and inter-character interactions. Empirical assessments of seven languages demonstrate considerable gains in both performance and processing speed, demonstrating RAMT's usefulness in bridging the resource gap in cross-lingual applications. Our findings demonstrate that this integrated technique promotes more equitable language processing solutions, paving the way for improved access and comprehension in low-resource linguistic environments.
46.	Investigating the design of ssPalmO-derived lipid nanoparticles for mrna delivery applications using molecular dynamics simulations A Barange, MN Luwang, **SK Meena** - ACS Omega, 2025 **Abstract:** The rational design of lipid nanoparticles (LNPs) is essential for the effective transport of drugs and genetic material, as their structural and dynamic properties are heavily influenced by lipid composition and functional group modifications. In this study, we employed molecular dynamics simulations with density functional theory (DFT) derived force fields to investigate the bilayer properties of ssPalmO lipids, their phenyl ester (ssPalmO-phe) and benzyl ester (ssPalmO-ben) derivatives, as well as their *cis* and *trans* isomers. While all systems formed stable bilayers, *cis*-ssPalmO deviated by adopting a flexible, nonlamellar architecture. *Trans* isomers of ssPalmO-phe and ssPalmO-ben exhibited greater bilayer thickness, packing density, and order parameters due to stronger intramolecular chain interactions, while their aromatic substituents reduced lateral diffusion relative to ssPalmO. *Trans* isomers exhibited lower electrostatic potential differences, which increased upon incorporation of helper lipids, concomitantly enhancing bilayer packing and thickness while suppressing diffusion. These results clarify how lipid functionalization, stereochemistry, and helper lipid composition modulate bilayer organization, offering molecular level guidance for rational LNP design in drug and mRNA delivery. 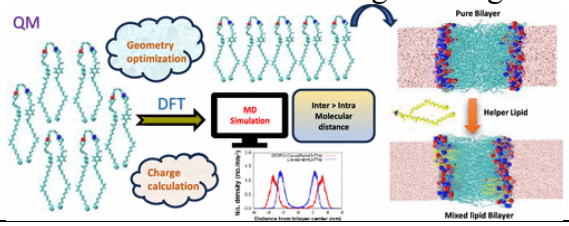
47.	Machine learning driven insights into yield strength of multi-principal element alloys **D Beniwal, A Kaushik, A Tiwari, PK Ray** - Journal of Materials Research, 2025 **Abstract:** In this work, we present a machine learning (ML) model for predicting the compressive yield strength of multi-principal element alloys (MPEAs). The model uses physical and thermodynamic alloy descriptors that capture various aspects of the alloying process such as lattice distortion, chemical interaction and intermetallic formation, and was used to explore yield strength variations in a variety of pseudo-ternary alloy systems viz. Zr_x-$(NbTa)_y$-$(MoW)_{1-x-y}$, W_x-Ti_y-$(HfNbTaZr)_{1-x-y}$ and $(MoNb)_x$-$(AlCr)_y$-$(FeNi)_{1-x-y}$ wherein it was validated along continuous composition pathways through comparison with experimentally observed yield strength values. The Compositional-Stimulus and Model-Response framework was used to decode the decision-making process of the ML model for obtaining alloy specific insights. Further, the model predictions were compared with hardness and phase predictions from other pre-trained ML models to establish consistency between different ML models. The model enables high-throughput screening for targeted yield strength and identifies key features for capturing yield strength variations in MPEAs.

	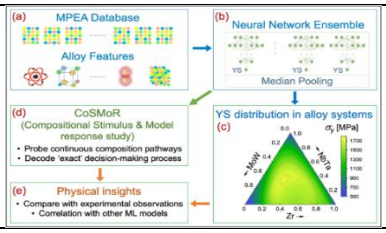
48.	Mechanistic understanding of origin of selectivity for oxygen evolution reaction in untreated natural seawater oxidation: Theoretical and experimental insights PV Raja, **DR Kanchan, A Banerjee**, A Joshy, R Sankannavar, I Mahesh - International Journal of Hydrogen Energy, 2026 **Abstract:** Direct seawater electrolysis is a promising approach for green hydrogen production, particularly for stakeholders in arid coastal regions. However, its large-scale implementation is hindered by the competing chloride ion oxidation reaction (ClOR) at the anode. This compromises oxygen evolution reaction (OER) selectivity and generates toxic and corrosive byproducts. However, although OER selectivity is known to depend on the kinetics of both competing reactions, as well as on the electrolyte pH and chloride ion concentration, the microscopic mechanistic understanding of how these parameters collectively influence selectivity remains largely unexplored. Here, we develop semi-empirical models to predict OER selectivity by incorporating Tafel kinetics of both ClOR and OER under different mechanistic scenarios. These models account not only for the aforementioned parameters but also reveal how selectivity is influenced by reaction pathways, and other various parameters. To validate the model, the OER selectivity of the transition metal phosphate electrocatalyst was quantitatively evaluated in various saline water electrolytes, including untreated natural seawater (collected from the Bay of Bengal in India), simulated seawater, and simulated brackish water. For comparison, benchmark noble metal catalysts (Ir/C and Pt/C) were also tested under identical conditions. Density functional theory calculations provided further mechanistic insights into these reactions. The experimental results were in good agreement with model predictions, with deviations attributable to dynamic pH shifts during natural seawater electrolysis and mass transfer resistance. This combined theoretical-experimental study provides mechanistic insights and design principles for advancing selective direct seawater electrolysis, offering a pathway toward efficient and sustainable hydrogen energy production. 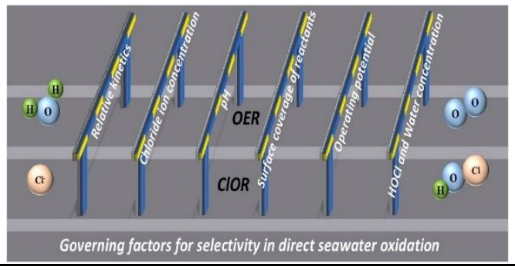
49.	MOT-STM: Maritime object tracking: A spatial-temporal and metadata-based approach VS Nageli, A Jamal, **P Goyal**, RKSS Gorthi - Image and Vision Computing, 2025 **Abstract:** Object Tracking and Re-Identification (Re-ID) in maritime environments using drone video streams presents significant challenges, especially in search and rescue operations. These challenges mainly arise from the small size of objects from high drone altitudes, sudden movements of the drone's gimbal and limited appearance diversity of objects. The frequent occlusion in these challenging conditions makes Re-ID difficult in long-term tracking.In this work, we present a novel framework, Maritime Object Tracking with Spatial–Temporal and Metadata-based modeling (MOT-STM), designed for robust tracking and re-identification of maritime objects in challenging environments. The proposed framework adapts multi-resolution spatial feature extraction using Cross-Stage Partial with Full-Stage (C2FDark) backbone combined with temporal modeling via Video Swin Transformer (VST), enabling effective spatio-temporal representation. This design enhances detection and significantly improves tracking performance

	in the maritime domain.We also propose a metadata-driven Re-ID module named Metadata-Assisted Re-ID (MARe-ID), which leverages drone's metadata such as Global Positioning System (GPS) coordinates, altitude and camera orientation to enhance long-term tracking. Unlike traditional appearance-based Re-ID, MARe-ID remains effective even in scenarios with limited visual diversity among the tracked objects and is generic enough to be integrated into any State-of-the-Art (SotA) multi-object tracking framework as a Re-ID module.Through extensive experiments on the challenging SeaDronesSee dataset, we demonstrate that MOT-STM significantly outperforms existing methods in maritime object tracking. Our approach achieves a state-of-the-art performance attaining a HOTA score of 70.14% and an IDF1 score of 88.70%, showing the effectiveness and robustness of the proposed MOT-STM framework.
50.	Mycobacterial and monkeypox homologous epitopes: Building blocks of a robust monkeypox vaccine **S Prajapati, JA Malik, T Lamba, MA Zafar, MA Khan, B Sangwan, S Nanda, JN Agrewala** - Journal of Biosciences, 2025 **Abstract:** Numerous scientific studies have established that the BCG vaccination reduces susceptibility to bacterial and viral infections, particularly those causing respiratory tract ailments. This effect is partly attributed to the cross-reactivity of BCG antigens, which reinforces immunity and presents an important avenue for therapeutic interventions against bladder cancer, Buruli ulcer, and leprosy. Remarkably, individuals residing in tuberculosis (TB)-endemic regions who have received BCG vaccinations exhibit a significant reduction in the incidence of monkeypox virus (MPV) infections. This observation could be attributed to shared T-cell and B-cell epitopes between mycobacteria and MPV, raising the possibility of eliciting cross-reactive immune responses. Such cross-reactivity could account for the enhanced protection conferred by the BCG vaccination against MPV infections. To explore this possibility, we employed advanced immunoinformatics tools. Our analysis successfully identified common CD4 T-cell, CD8 T-cell, and B-cell epitopes shared between MPV and mycobacteria. Notably, the T-cell epitopes demonstrated high immunogenicity and substantial affinity, with promiscuous binding to multiple human leukocyte antigen (HLA) class I and class II alleles, indicating the potential for these epitopes to trigger robust immune responses. Indeed, the predicted outcomes encompassed the induction of Th1-cell and Th2-cell responses via the predicted epitopes. These findings carry profound implications. They imply that prior exposure to cross-reactive mycobacterial antigens during recent pandemics could have contributed to increased levels of protection against MPV infections in TB-endemic regions, in contrast to areas non-endemic for TB. The identified T-cell and B-cell epitopes may thus serve as promising candidates for developing vaccines to combat MPV and mitigate its spread.
51.	*N*-annulated indenofluorene: An isomeric motif for *N*-annulated perylene **HK Saha,** Tarun, D Mallick, UK Pandey, **S Das** - Organic Letters, 2025 Abstract: *N*-Annulated indenofluorene (**NIF**), a structural isomer of the well-known *N*-annulated perylene (**NP**), has been synthesized. While the band gap of **NP** is larger than that of perylene, the band gap of **NIF** (1.40 eV) is smaller than that of parent indeno[2,1-*c*]fluorene (1.60 eV) due to the inclusion of a nearly planar 8π azepine ring in the π-conjugated backbone, enhancing the core antiaromaticity. The ground state properties are evaluated by structural (single-crystal) and spectral (NMR, UV–vis–NIR, and CV) analyses and supported by computations (NICS and ring current). **NIF** is an ambipolar material with good electron mobility (1.58×10^{-3} cm^2 V^{-1} s^{-1}) and high hole mobility (1.79×10^{-2} cm^2 V^{-1} s^{-1}), surpassing the hole mobility of the unipolar **NP** isomer.

	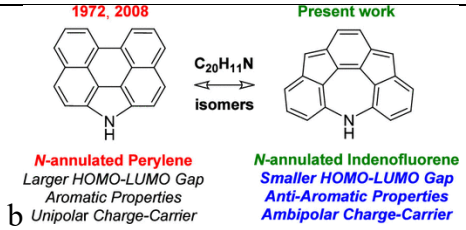
52.	On characterization of Monogenic number fields associated with certain quadrinomials and its applications **T Chatterjee, K Kumar** - Research in Number Theory, 2026 **Abstract:** Let f(x)=xn+ax3+bx+c be the minimal polynomial of an algebraic integer θ over the rationals with certain conditions on a, b, c, and n. Let K=Q(θ) be a number field and OK be the ring of integers of K. In this article, we characterize all the prime divisors of the discriminant of f(x) which do not divide the index of Z[θ] in OK. As an interesting corollary, we establish necessary and sufficient conditions for Z[θ] to be integrally closed. Finally, we investigate the types of solutions to certain differential equations associated with the polynomial f(x).
53.	On the size of the Fourier coefficients of Hilbert cusp forms **B Kumar** - The Ramanujan Journal, 2026 **Abstract:** Let f be a primitive Hilbert cusp form of weight k and level n with fourier coefficients cf(m). We prove a non-trivial upper bound for almost all Fourier coefficients cf (m) of f. This generalizes the bounds obtained by Luca, Radziwiłł and Shparlinski. We also prove the existence of infinitely many integral ideals m for which the Fourier coefficients cf (m) have the improved upper bound and further we obtain a refinement of these integral ideals in terms of prime powers. In particular, this enables us to deduce the bound for Fourier coefficients of elliptic cusp forms beyond the 'typical size'. Moreover, we prove further improvements of the bound under the assumption of Littlewood's conjecture. Finally, we study a lower bound for the Fourier coefficients at prime powers provided the corresponding Hecke eigen angle is badly approximable.
54.	Optically excited nano-mechanical modes of a droplet B Singh, Amarnath, N Kumawat, **M Mishra, KC Jena,** KP Singh - Optics Letters, 2025 **Abstract:** We show that a surging radiation pressure excites welldefined nanoscale optomechanical discrete modes of a sessile droplet. Using a pump-probe approach, we isolate growth and damped oscillations of droplet modes from background evaporation and steady-state bulge. For a microlitre droplet, we find that the amplitude of a mode increases linearly with the rate of pump power surge, reaching ~ 20 nm for 2.7 kW/s. The mode frequency is characteristic of droplet geometry and physical properties but independent of the optical excitation. A Navier–Stokes model of droplet for realistic parameters reproduces the key experimental results. Furthermore, we show phenomenon of frequency splitting for the n = 3 mode of non-spherical droplets. This work opens a route to probe nanoscale shape oscillations of complex droplets subjected to spatiotemporally structured stimulus.
55.	Performance of biaxial voided reinforced concrete slabs under air-blast loading: Experimental investigation and non-destructive assessment **AK Chaudhary, S Muthulingam,** D Kothari - Structures, 2025 **Abstract:** Advancing blast-resistant concrete systems is essential for overcoming the limitations of conventional slabs and enhancing structural resilience under extreme loading. This study experimentally examines the blast response of biaxially voided reinforced concrete slabs subjected to air-blast loading. Spherical void formers were strategically embedded within two-way reinforced concrete slabs, which were exposed to a 1 kg TNT charge at a scaled distance of 0.5 m/kg$^{1/3}$. The dynamic behavior was monitored using strain gauges and pressure transducers, while post-blast integrity was assessed through non-destructive tests such as rebound hammer and ultrasonic pulse velocity tests. Results revealed a distinctive successive two-peak compressive

	strain profile, attributed to incident and reflected stress waves, with localized strain amplification observed around the voids. Despite these localized effects, the slabs exhibited neither full-depth penetration nor structural collapse. Damage mapping indicated non-uniform, highly localized cracking, and non-destructive evaluation showed a moderate reduction in concrete strength and up to 50 % decrease in UPV velocities in affected zones. The central region sustained the most damage, yet the computed damage indices confirmed that the slab retained serviceable load capacity. These findings demonstrate that the incorporation of voids substantially altered wave propagation and enhanced energy dissipation, preventing catastrophic failure and suggesting a promising approach for lighter blast-resistant slabs.
56.	Practicalities to communication receiver for JSC waveform: Whether to filter or to undersample? **D Salwan, S Agarwal, B Kumbhani** - IEEE Communications Letters, 2025 **Abstract:** In this letter, we consider low-complexity symbol detection schemes for the UAV communication receiver using a phase shift keying-linear frequency modulated (PSK-LFM) joint sensing and communication (JSC) waveform. The JSC waveform typically employs a large bandwidth as it helps in performing radar functionality. However, UAV communication receivers typically operate at a much lower bandwidth as compared to radar. Therefore, this letter presents a communication receiver performance for two schemes: one that filters and samples a portion of the signal, while the other undersamples the entire received signal for bit detection. We analytically derive BER expressions for both schemes under imperfect CSI and assess their performance. The results show that undersampling provides better BER performance than with filtering at the same sampling rate, highlighting the robustness of the proposed receiver design.
57.	Progress in the design and development of thermoelectric generator heat recovery systems: A comprehensive review **R Goswami, R Das, S Ganguly…** N Miljkovic - Renewable and Sustainable Energy Reviews, 2026 **Abstract:** The global energy transition emphasizes emission reduction, energy efficiency, and renewable integration. However, according to the second law of thermodynamics, all energy conversion systems inherently lose a portion of input energy as waste heat, representing a vast, underutilized resource for sustainable power generation and efficiency enhancement. Earlier studies focused solely on material-specific advancements or single-source applications. This study provides a comprehensive and integrative assessment of thermoelectric generator (TEG) heat recovery systems, encompassing artificial intelligence (AI) and machine learning (ML)-assisted materials design, techno-economic analysis, multi-physics modeling, dynamic system performance under different feasible heat sources, critical challenges and future approaches. The review begins with an in-depth assessment of diverse waste heat sources, including solar ponds, photovoltaic cells, cookstoves, biomass gasifiers, automotive engines, and industrial processes. It highlights suitable semiconductor materials across broad temperature ranges and systematically discusses recent advancements in TEG systems design, optimization, and performance enhancement for efficient waste heat recovery. The performance of TEGs highlights that Bi_2Te_3-based compounds remain ideal for low temperature heat sources while PbTe, skutterudites, and Mg_3Sb_2 alloys perform efficiently with mid-temperature sources. Integration of AI/ML, and multiphysics simulation has accelerated design optimization, improved prediction accuracy, and reduced computational cost. Hybrid configurations of TEGs with photovoltaic cells, biomass-driven systems, and automotive engines demonstrate strong potential in improving fuel efficiency, reducing emissions, and enhancing energy utilization. Despite the inherent advantages, commercialization remains limited by material costs and moderate conversion efficiencies. Therefore, future research needs to focus on scalable manufacturing, recyclable and non-toxic materials, and hybrid system integration. Aligning with circular economy principles, next-generation TEG systems will contribute significantly to global decarbonization and sustainable energy transitions. This review offers a unified roadmap connecting scientific, engineering, and economic insights toward real-life deployment of efficient, durable, and eco-friendly TEG technologies.

58.	Reverse-bias driven anomalous polarity switching in FeSi2/Ga2O3-NRs heterojunction based solar-blind photodetector **R Dahiya, D Kaur,** X Zhang, **BP Gatadi**…**M Kumar** - Applied Surface Science, 2025 **Abstract:** Recently, polarity-switching photodetectors have attracted significant attention due to their ability to reverse photocurrent direction based on the incident light wavelength or applied bias. This unique functionality makes them promising for applications in optical logic operations, optically controlled artificial synapses, and dual-channel communication. Most of the reported polarity-switching devices have a wavelength dependent switching, while voltage-driven switching is rare to find, especially for narrowband devices such as those used for secure UV-C communications. In this work, we present a $FeSi_2/Ga_2O_3$-NRs heterostructure photodetector that demonstrates polarity-switching behavior only under an applied reverse bias. Under 254 nm illumination, the device exhibits a photocurrent direction change from negative to positive, offering a novel approach for encrypted solar-blind detection. The band alignment analyzed via X-ray photoelectron spectroscopy (XPS) and Kelvin probe force microscopy (KPFM) is used to understand the underlying working mechanism. Additionally, the device exhibits high stability in performance even after 1 year of ambient storage without encapsulation. The demonstrated polarity-switching behavior in this solar-blind photodetector provides a pathway for encrypted optical signal processing and secure UV-C imaging with minimal background noise in the ambient condition. 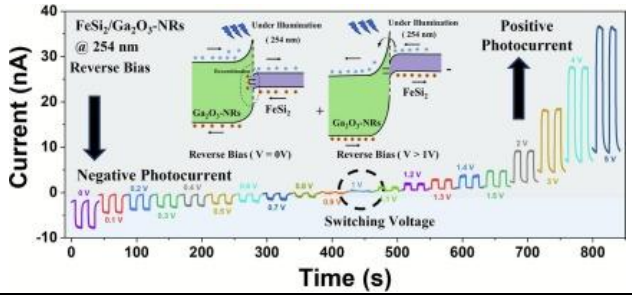
59.	Selective laser melting of Al_2O_3-EIP composite: Single track study **S Rathor, M Altaf, S Yadav, R Kant,** P Kumar - Lasers in Engineering (Old City Publishing), 2025 **Abstract:** This work includes a single-track study of Alumina (Al_2O_3)-Electrolytic Iron Powder (EIP) composites in different weight percentage compositions using the selective laser melting (SLM) process. This experimental study aims to find the feasibility of Alumina and EIP composites at different wt.% composition at fixed process parameters. It specifically involves powder preparation through ball milling, tracking the morphology, element mapping of the layer at different Alumina compositions, microhardness, and scratch test results, which are discussed at the end. The outcomes relate the microhardness with different weight compositions of Alumina quantitatively. The element mapping confirmed the presence of composite powder and showed the separate substrate at the interface. A scratch test was also performed, and it was found that the single layer resistance against abrasion and scratches at different percentage compositions of Alumina when subjected to ramp loading.
60.	Stress driven pore to wrinkle transition in low energy ion irradiated polydimethylsiloxane (PDMS) films **P Kumar, S Sarkar** - Applied Surface Science, 2025 **Abstract:** Polymeric surfaces patterned at the micro and nano scale hold significant potential for emerging technologies such as flexible electronics, biosensors, optical devices, and biomedical platforms. In this study, we investigate the evolutionary transitions of surface patterns on polydimethylsiloxane (PDMS) under low-energy argon ion beam irradiation, focusing on the transformation from porous structures to wrinkled morphologies. Ion-induced blistering arising from volatile species accumulation and defect agglomeration in the subsurface region results in a porous morphology. With prolonged irradiation, the buildup of compressive stress in the ion-

	stiffened surface layer relaxes through strain-driven buckling against the compliant polymer substrate, giving way to a tunable ion beam parameter dependent wrinkled texture from the initial pore-laden topography. Our study demonstrates that broad beam ion irradiation offers a controllable, single-step pathway for generating and tuning porous-wrinkle surface architectures in polymeric materials without extrinsic contamination by manipulating the competing surface mechanisms involved. Power spectral density analysis identifies surface diffusion as the dominant mechanism governing pattern evolution, while X-ray photoelectron spectroscopy verifies the formation of a silica-like layer confined to the ion penetration depth. Collectively, these results demonstrate a robust pathway for controlled surface patterning with tunable morphology and periodicity, paving the way for diverse technological applications. 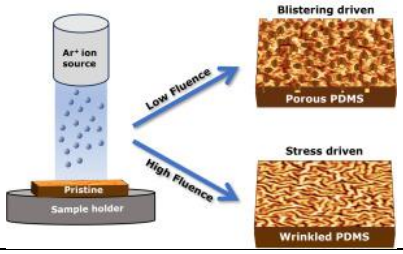
61.	Structure and strength of a highly stable eight-element BCC refractory high entropy alloy **N Bibhanshu, P Kumar**, RK Ray, S Suwas - Journal of Alloys and Compounds, 2025 **Abstract:** In an attempt to develop a stable, single-phase Refractory High Entropy Alloy (RHEA), containing more than five elements, five equiatomic RHEAs, such as NbCrTiTa, NbCrTiMoVTa, NbCrTiAlMoVTa, NbCrTiMoVHf, and NbCrTiMoVTaWMn, were prepared using vacuum arc melting. Phase investigation, carried out by the X-ray diffraction, revealed that although the matrix structure is generally BCC type for all five RHEAs, the 8-element NbCrTiMoVTaWMn RHEA possesses a perfect BCC single-phase structure. The stability of all five BCC RHEAs was investigated via differential scanning calorimetry (DSC), which indicated that the single-phase BCC 8-element RHEA is stable up to the temperature of 1400 °C. Further, the DSC results also showed an endothermic behavior of this alloy with the increase of temperature, which can be taken as a sign of increased stability on heating. This has been further confirmed on the basis of high-temperature XRD measurements, which showed a variation in interplanar d-spacings on heating. Detailed analysis of diffraction line profiles suggests an expansion of the lattice till 1000 °C, followed by a contraction thereafter. Additionally, an asymmetric contraction has been observed after thermal exposure, as revealed by the changes in the interplanar spacings of the (110), (200), and (211) planes. The mechanical strength of the developed 8-element RHEA, which is of the order of ~1.7 GPa at room temperature, is found to be higher compared to all reported single-phase BCC RHEAs, and the higher strength of this alloy is steadily maintained over a wide temperature range, as compared to the other alloys. 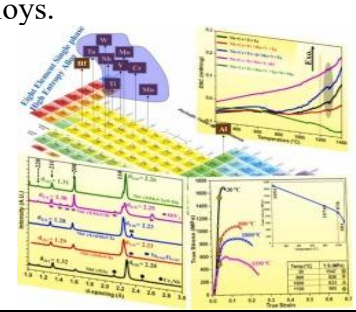
62.	Surface morphology transformations after sequential laser treatment during turning of mild steel N Deswal, **R Kant,** S Yadav, P Kumar - Lasers in Engineering (Old City Publishing), 2025 **Abstract:** Surface morphology of a final product has been the primary focus of any product to achieve better part performance and durable life. Surface morphology is affected by several factors such as friction, heat generation, interaction between the cutting tool and the workpiece surface, etc. The present article aims to investigate the surface morphology of mild steel during the sequential turning and laser post treatment processing. Cutting speed, laser power, and laser spot

	diameter have been varied to analyze the surface roughness and machined surface damage during the conventional turning (CT) process and sequential post-processing via laser. The surface roughness and machined surface damage are found to be higher for the sequential post-processing via laser than the CT process for most of the conditions. However, for certain cases, the surface roughness and machined surface damage are observed to be lower for sequential post-processing via laser than the CT process.
63.	Sustainable application of edible solute to control reservoir evaporation loss **I Dhada, Poonam**, S Singha, AK Shukla - Scientific Reports, 2025 **Abstract:** Recently, water preservation globally, particularly in Indian cities, has been prominently featured in newspaper headlines, underscoring its importance. This research explores the innovative use of edible solutes to tackle the challenges of evaporation in reservoirs, including water loss, increased salinity, and ecological disruptions. Traditional methods for controlling evaporation often have environmental drawbacks and high operational costs. By evaluating the environmental impact, cost-effectiveness, and feasibility of edible solutes such as mustard oil, neem oil, til oil, castor oil, cetyl alcohol, and stearyl alcohol, this study investigated their sustainable application in eight reservoirs across Andhra Pradesh and Telangana states in India. Through break-even analysis, the economic viability of edible solutes is compared to that of conventional methods over the lifespan of a reservoir. These findings suggest that edible solutes offer a promising and environmentally friendly alternative, reducing evaporation rates while minimizing the adverse effects on water quality and ecosystems. Despite the initial investment costs, the long-term savings and environmental benefits surpass those of the conventional approaches. This study estimated evaporation rates for eight reservoirs across Andhra Pradesh and Telangana in India (3049 mcm of water/year), showing a significant reduction when cetyl alcohol was used as a solute. Cetyl and stearyl alcohols are highlighted as practical and cost-effective evaporation retardants. Considering the cost of water at one *paise* per five litres of saved water, the break-even point (BEP) analysis for the adopted scenarios reveals that BEP is achieved for 30%, 10%, and 5% reduction in evaporation within one, two, and three months, respectively. Similarly, for scenario II (one paisa per one litre of saved water), the BEP was achieved at the beginning, 1.5 months, and 2.5 months, considering evaporation reduction by 30%, 10%, and 5%, respectively. Future research should validate the efficacy of microfilms in mitigating evaporation using time-resolved interferometry techniques. This study advocates sustainable water management practices and provides valuable insights for policymakers, water resource managers, and stakeholders seeking efficient solutions for evaporation control in reservoirs.
64.	Tailoring nanoparticle surfaces empowered by multivariate techniques for detection of multiple antibiotic fingerprints in real samples using hand-held colorimetric signal redout **Ranbir,** G Singh, N Kaur, **N Singh** - ACS applied materials & interfaces **Abstract:** Due to the complex and varied toxicological characteristics exhibited by different antibiotics, which present significant risks to both the environment and human health, there is an urgent requirement for highly efficient sensors capable of detecting antibiotics. The present study introduces a straightforward yet efficient colorimetric sensor array comprising surface-tailored nanoparticles, analyzed using different techniques including dynamic light scattering, zeta potential, Fourier transformation infrared spectroscopy (FTIR), X-ray photoelectron spectroscopy, atomic force microscopy, field emission scanning electron microscopy, and high resolution transmission electron microscopy for identifying and discriminating antibiotics. Each antibiotic exhibits distinct binding affinities toward these sensing elements, leading to varied colorimetric and UV–visible absorption response patterns, which lead to unique “fingerprints” associated with each antibiotic. These patterns are quantitatively distinguishable through linear discriminant analysis, decision tree algorithm, random forest algorithm, support vector machine, and hierarchical clustering analysis. With 100% accuracy, the sensor array successfully discriminates between eight antibiotics (amoxicillin, azithromycin, neomycin, streptomycin, chloramphenicol, ofloxacin, fluconazole, and ciprofloxacin), with detection limits ranging from 1.7 to 8.3 μM. Additionally, binary and ternary mixture ratios of various antibiotics have also been successfully

	discriminated. Further, for the real-time applications, we have developed prototypes for colorimetric analysis and also modified the previously developed 96-well plate reader, which functions similarly to the UV–visible absorption spectrophotometer. These on-site sensing methods, with straightforward preparation, quick response, exceptional sensitivity, and consistently stable high-throughput signal output, show significant potential for practical use in food forensics and for environmental remediation. 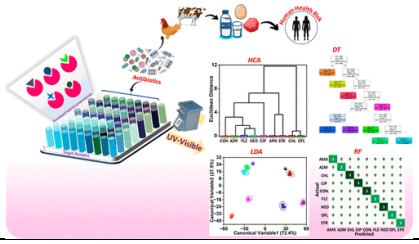
65.	Temperature-driven evolution of phonon-coupled carrier dynamics in lanthanum hexaferrite probed by terahertz spectroscopy: Implications for THz photonics S Biswas… **G Kumar,** P Dobbidi - Journal of Applied Physics, 2025 **Abstract:** Carrier-phonon coupling plays a central role in charge transport, energy relaxation, and device stability in the terahertz (THz) regime, making its investigation crucial for condensed-matter physics and future high-frequency technologies. We report a systematic study of the temperature-dependent THz time-domain response of lanthanum hexaferrite ($LaFe_{12}O_{19}$, LaM) across 296-683 K. Increasing temperature produces a clear decrease in transmission amplitude and a corresponding increase in time delay, highlighting the strongly dispersive nature of LaM. The reduction in transmission and enhanced absorption at elevated temperatures are linked to intensified phonon-carrier interactions and disorder-induced scattering. A nonlinear change in the refractive index indicates enhanced ionic polarizability from thermally activated lattice vibrations. At room temperature, LaM shows a high dielectric constant ($\varepsilon' \approx 13.9$ at 1 THz) and low dielectric loss ($\tan \delta \approx 0.03$ at 1 THz), dominated by ionic polarization. Temperature- and frequency-dependent optical conductivity trends provide direct evidence of carrier scattering and phonon coupling. Lorentz oscillator fitting of permittivity and conductivity confirms phonon-assisted resonances with temperature-driven shifts in resonance frequency, oscillator strength, damping, scattering time, and quality factor. These findings demonstrate the strong influence of carrier-phonon interactions on LaM's THz response and its promise for tunable THz devices.
66.	Time-dependent solvothermal synthesis of melamine cyanurate and melamine diborate: experimental and theoretical insights Ankita, Z Zhang, K Leifer, J Hilborn, D Li, J Zhu, **R Ahuja,** W Luo - Physical Chemistry Chemical Physics, 2026 **Abstract:** This study introduces a time-dependent solvothermal synthesis of hydrogen-bonded melamine cyanurate and melamine diborate at 180 °C, offering precise control over their framework compositions and structures through reaction time. The selective formation of melamine diborate and melamine cyanurate is achieved using the same set of precursors with cyanuric acid generated in situ from melamine hydrolysis. The phase composition varies with the reaction time, as confirmed by Fourier transformed infrared (FTIR) and X-ray photoelectron spectroscopy (XPS), which reveal the structural progression of these frameworks. Our synthesis method allows melamine cyanurate to nucleate or grow on melamine diborate crystals adopting a more crystalline rod-like morphology with clearer texture. Density functional theory (DFT) enhances the understanding of their electronic structures, highlighting core-level binding energy shifts (N 1s and B 1s) and the chemical activity of lone pair electrons, with the mixture of π and σ bonds playing a key role in determining the bandgaps. This proposed synthesis method enables precise tuning of hydrogen-bonded framework compositions providing valuable insights for material synthesis and structural design.
67.	Traffic dynamics in mixed connected and human-driven vehicle systems under visual angle effect M Verma, **AK Gupta,** S Sharma - The European Physical Journal Plus, 2025

	Abstract: The visual angle plays a pivotal role in the driving dynamics of connected vehicles (CVs) and human-driven vehicles (HDVs), influencing the overall stability of traffic flow. In a mixed traffic environments, the interactions between CVs and HDVs are primarily governed by perception-based dynamics, where each vehicle proceeds according to its perception of surrounding traffic conditions. To investigate this, a novel lattice hydrodynamic model is introduced to effectively study how visual angle impacts traffic dynamics in scenarios involving both CVs and HDVs. The traffic flow behavior is analyzed through linear stability analysis, where the neutral stability conditions are derived. Also, mKdV equation is attained near the critical point utilizing reduction perturbation technique. It is observed that as visual angle coefficient of human-driven and connected vehicles increases, the traffic flow becomes more stable. The numerical simulations are conducted to validate theoretical results. Further, based on power spectrum analysis, the spectral entropy is calculated, which reveals that the visual angle and the fraction of CVs positively impact the traffic flow stability. Additionally, the fluctuation patterns of average fuel consumption under the influence of these factors are systematically examined.
68.	Transesterification-derived biodiesel: A comprehensive assessment of feedstock diversity, engine performance, and pathways to sustainable transportation D Kumar, S Pratap, N Gupta, P Tyagi, **P Kumar,** RK Prajapati… - Discover Sustainability, 2025 **Abstract:** The escalating global energy demand and environmental degradation driven by fossil fuel consumption necessitate urgent transitions to sustainable alternatives. This comprehensive review examines biodiesel production via the transesterification route, emphasizing feedstock diversity, catalyst efficacy, and the physicochemical properties of biodiesel that influence diesel engine performance and emissions. First- to fourth-generation biofuels are critically analyzed, emphasizing the advantages of non-edible feedstocks such as Jatropha and algae, along with the use of efficient heterogeneous catalysts like CaO and KF/CaO. These catalysts enable high biodiesel yields, achieving up to 82.3% from Jatropha carcass oil and 69.3% from Karanja oil, while simultaneously minimizing food-security concerns. The basic properties of biodiesel such as viscosity, density, cetane number, and iodine value have a direct bearing on combustion efficiency, emission rates, and low temperature performance. Engine test result indicated that biodiesel blends are more environmentally friendly than fossil diesel as they significantly reduce carbon dioxide and hydrocarbon emissions. Although the higher oxygen content of biodiesel contributes to more complete combustion, it can also result in a moderate increase in nitrogen oxide (NOx) emissions. Among various feedstocks, rapeseed and algal biodiesels demonstrate an optimal balance between emission reduction and thermal efficiency, making them promising candidates for practical applications. In contrast, biodiesels derived from feedstocks with elevated cloud points, such as mustard oil, exhibit poor low-temperature flow properties, which can limit their suitability in colder climates. Overall, this study reaffirms the potential of transesterification-derived biodiesel as a sustainable and efficient alternative to conventional diesel, provided that feedstock selection, catalyst formulation, and emission mitigation strategies are effectively integrated within regional energy and environmental policy frameworks.
69.	Unveiling hidden perspectives: Examining COVID-19 impact on non-perennial river flow across ungauged river segments and anthropogenic footprint on the hydrological cycle **T Prashanth, S Ganguly** - Journal of Hydrology: Regional Studies, 2025 Abstract: Study region: Pennar River Basin, India. Study focus: The COVID-19 pandemic offered a one-of-a-kind opportunity to examine how the ecosystem reacts to diminished human interference. This study examines the rejuvenation potential of the ungauged lower Pennar River, India, between pre and post-COVID. Satellite-derived bathymetry (SDB) models are developed to estimate flow depth for ungauged river segments. Meteorological drought is assessed using the standardized potential evapotranspiration index (SPEI) and the standardized precipitation index (SPI), whereas groundwater drought is evaluated using the standardized groundwater table index (SGWTI). The correlation between SPEI, SPI, and SGWTI is employed to ascertain that groundwater drought influences river cross-section due to anthropogenic or natural forcings. The

	newly proposed index of river rejuvenation susceptibility (RRS) is assessed by integrating weights derived from the Analytical Hierarchy Process (AHP) and Fuzzy AHP with the magnitude of the aforementioned indices. New hydrological insights for the region: The findings indicate a low to moderate correlation between the SPEI, SPI and SGWTI, emphasizing that groundwater drought in the study area is attributable to human interventions such as pumping. The fact is cross-validated using the stage of extraction data. The RRS of the lower Pennar River is identified to have increased considerably during COVID-19 due to a significant reduction in groundwater extraction, as proven by depth-duration curves and standardized total water storage anomalies (STWSA). 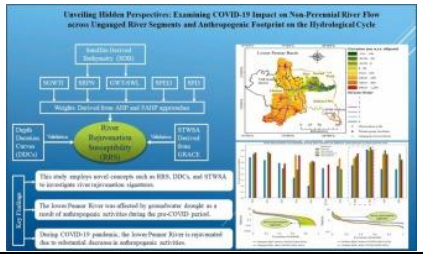

Disclaimer: This publication digest may not contain all the papers published. Library has compiled the publication data as per the alerts received from Scopus and Google Scholar for the affiliation “Indian Institute of Technology Ropar” for the month of December, 2025. The author(s) are requested to share their missing paper(s) details if any, for the inclusion in the next publication digest.